Available online at www.sciencedirect.com
ScienceDirect
Journal of Environmental Sciences 19(2007) 367–373
JOURNAL OF ENVIRONMENTAL SCIENCES
ISSN 1001-0742
CN 11-2629/X
www.jesc.ac.cn

A new photon kinetic-measurement based on the kinetics of electron-hole pairs in photodegradation of textile wastewater using the UV-H_2O_{2FS}-TiO_2 process

SHIGWEDHA Nditange[1], HUA Zhao-zhe[1,2,*], CHEN Jian[1,2,*]

1. Laboratory of Environmental Biotechnology, School of Biotechnology, Southern Yangtze University, Wuxi 214036, China
2. Key Laboratory of Industrial Biotechnology, Ministry of Education, Southern Yangtze University, Wuxi 214036, China. E-mail: huazz@sytu.edu.cn; jchen@sytu.edu.cn

Received 23 March 2006; revised 10 May 2006; accepted 29 May 2006

Abstract

Actual textile wastewater and synthesized wastewater containing various textile dyes were photocatalytic degraded by the UV-H_2O_{2FS}-TiO_2 process in an annular-flow photocatalytic reactor. In this process, a photon kinetic-measure was adopted to obtain constant rates of dyes decomposition. It was theorized that, by illumination at different UV frequencies, the electrons within the semiconductor were excited from the valence band to the conduction band, yielding the formation of electron-hole pairs which are the pre-requisites for photocatalysis. CPT (critical photonic time) exposure required to cause 90% of vibrations between the double and single bonds along the molecular chain of the dyes to be oxidized, was taken to measure the photocatalytic activities. The CPTs varied with the frequencies of the UV spectral areas. The derivatization of CPT from the first-order kinetic law was presented.

Key words: critical photonic time (CPT); photon efficiency; UV frequencies; regression line; textile wastewater

Introduction

Textile industries are the largest consumers of organic dyes, and it is expected that 10%–15% of the dye is lost during the dyeing process and is released as effluent. These compounds, however, are usually recalcitrant, retain structural integrity or show very low degradation kinetics for conventional biological processes. The final effluents (after treatment) still have very intense coloration (Bahorsky and Bryant, 1995; Wu *et al*., 1996; Kunz *et al*., 2001). They are also designed to resist photodegradation (Forgacs *et al*., 2004). However, in the UV-H_2O_{2FS}-TiO_2 process, the rate of dye decomposition is rapid and final effluent is clear (Shigwedha *et al*., 2006).

In the latter photocatalytic process, the semiconductor was immobilized in a thin film. On illumination at appropriate UV frequencies, the electrons within the semiconductor were excited from the valence band to the conduction band, yielding the electron-hole pairs, which are the pre-requisites for photocatalysis. The photogenerated holes within TiO_2 can directly induce oxidation or undergo charge transfer with an absorbed water molecule, ultimately leading to the formation of HO· radicals (E^0 = 2.80 V). The reactions of this electron-hole pair with a variety of electron acceptors and donors and the electron-hole recombination processes have been well studied (Rothenberger *et al*., 1985; Fox, 1991).

TiO_2 photocatalyst in an immobilized form is economical, exhibit high stability in aqueous solutions, no photocorrosion under band gap illumination. And it also has shown exceptional surface properties for the treatment of effluents at a larger scale (Arabatzis *et al*., 2002; Noorjahan *et al*., 2003; Shigwedha *et al*., 2006). We hypothesized that the presence of H_2O_2 from the start (H_2O_{2FS}) would improve the photocatalytic degradation at a constant rate. That improvement in photocatalytic degradation was more important to measure the kinetics of electron hole pair than the concentration of the dyes. If this is the case, the presence of H_2O_{2FS} should speed up the photocatalytic process because: (1) it prevents electron holes recombination; (2) it prevents electron band competition; (3) it enhances the formation of extra H_2O_2 and its decomposition; (4) it serves as initiator of radical reaction, oxygen source and accelerates the photodegradation processes; (5) in combination with immobilized TiO_2, it makes the photocatalytic measurements simple and overall conversions constant; (6) it does not destroy the immobilized photocatalyst; (7) it should reduce the film-diffusional resistance too.

Literature contains the use of relative photonic efficiencies as a means of comparing photochemical processes (Tahiri *et al*., 1996; Serpone *et al*., 1996; Malato *et al*., 2000). Other concept of global photonic efficiency that relates mineralization and initial degradation rate introduced by Medina-Valtierra *et al*. (2005), has been adapted from relative photonic efficiency to complement the comparison of process efficiencies with different photocatalysts

Project supported by the Scientific Research Foundation Funded for the Returned Oversea Scholars, State Education Ministry of China (No. 2055-55). *Corresponding author. E-mail: huazz@sytu.edu.cn; jchen@sytu.edu.cn.

under the same experimental conditions. These methods avoid knowing the amount of photons absorbed by the photocatalyst and attenuate other unidentified aspects in general. However, in other studies variations with respect to the absorbed photon flux were considered (Wang *et al*., 2002a). Some researchers recommend using formal rate constants in the photodegradation of organic substrates as a measure of the photo-oxidation efficiency (Sabin *et al*., 1992).

In order to measure kinetics, we chose to measure the CPTs (critical photonic times). The rate of formation of electron hole pairs can be predicted from the CPTs during the photocatalytic degradation of the dyes in water. The CPTs are times of UV exposure required to cause 90% of oscillations between the double and single bonds along the molecular chain of the dyes to be oxidized. This kinetic-measure was chosen because we have observed that when the concentration of the dyes in water is of the order of or less than 70 mg/L, there is no remarkable difference between the dye concentration in the bulk fluid and on the photocatalyst surface, thereby reducing the rate of decolorization significantly. As the CPT procedure does not require identification of the dyes in the effluent, this leads us to kinetically analyze the kinetics process of the photocatalytic reactions regardless of the structure and concentration of collective dyes in the textile effluent before treatment. The derivatization of CPTs in the present work predicts the kinetics of dye decomposition of a wide variety of the textile dyes resulting from a much wider range of UV frequencies than has been done in the previous works. The equations based on CPTs successfully predicted the efficiency of the UV frequencies in the cases tested.

1 Experimental

1.1 Reagents and light sources

A 30% (v/v) H_2O_2 solution (laboratory reagent grade) was purchased from Shanghai Chemicals Reagent Company. A Pyrex glass tube (photocatalytic surface area, 0.0123 m^2) coated with a transparent thin film of anatase TiO_2 was provided by Kyushu Institute of Technology, Japan. The five monochromatic UV lamps (6 W each) used as light source were: (1) a black light blue fluorescent lamp (BL-B) with wavelength of 389 nm (FL6 BL-B, Matsushita Electric Industrial Co. Ltd., Osaka); (2) a blue-light fluorescent lamp (UV-B) with a wavelength of 313 nm (S8T4B, Jiangyin UV Development Electric Co., Wuxi); (3) a germicidal lamp (GL-6) with a wavelength of 254 nm (GL 6, Sankyo Electric Co., Tokyo); (4) a germicidal lamp (UV-C) with a wavelength of 222 nm (S212T3, Jiangyin UV Development Electric Co., Wuxi); and (5) a vacuum lamp (O_3-L) with a wavelength of 185 nm (Jiangyin UV Development Electric Co., Wuxi).

1.2 Photocatalytic reactor system and its operating method

The photocatalytic reactor (Shiraishi *et al*., 2003), a reservoir and a peristaltic pump (BT00 600M; Lange Electric Co.) were connected in a loop and recirculated in a batch recirculation closed system as shown in Fig.1. Decolorization kinetics analysis was performed on 400 ml of each treatment at natural pH values (ranged from 6.54 to 9.63). The pH of the solutions was measured with a PHS 2C accurate pH meter. The solution pH was adjusted to the desired value by addition of sodium hydroxide or sulfuric acid. However, pH values of test solutions used in this study were not adjusted to any value. The photocatalytic decomposition of the dyes and the corresponding decolorization process were basically controlled by the natural pH of the wastewater. The decolorization rate of the dyes, using the CPTs at initial pH (6.0–9.6) and adjusted pH to 6.5 conditions were studied. Maximum decolorization for all the treatments studied in this work was observed at a natural pH ranges and the decolorization rates decreased at adjusted pH. Although both the individual and mixtures of the dyes in aqueous solutions were decolorized at pH range of 6.5–6.8, actual textile effluents were mostly decolorized at around pH 9.6. On the other hand, an attempt to adjust the pH from 9.6 to 6.5 resulted in significantly slower decolorization, based on the CPTs principles. These observations indicate that the optimum pH for the UV-H_2O_{2FS}-TiO_2 process depends on the composition of the original substrates in wastewater treated as observed and reported elsewhere (Shigwedha *et al*., 2006). The explanation of the adjusted pH effect on the rate of decolorization could be due to the medium of pH, which is expected to affect the ionization state

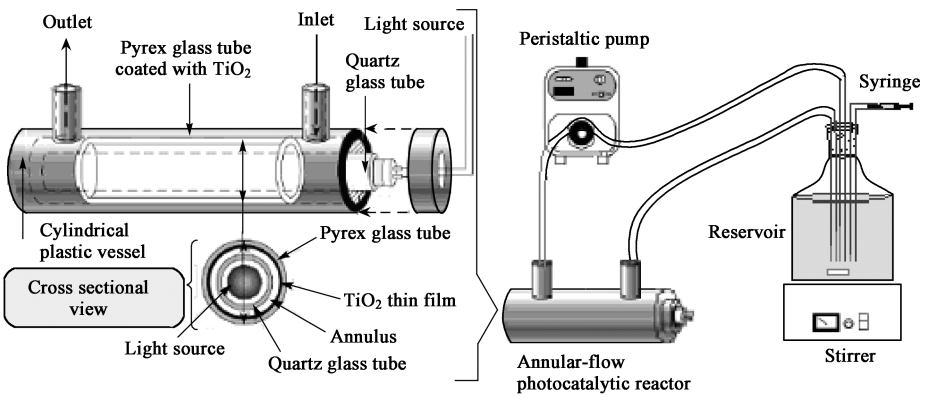

Fig. 1 Annular-flow photocatalytic reactor and its batch recirculation system.

of the functional groups on the TiO_2 thin film. Other entrapped substrate ions (sulfates, carboxylic, sodium and amino groups) are likely to adsorb to TiO_2 thin film thus bringing it into close contact with hydroxyl radicals. The colored solutions, dosed with 1 ml of H_2O_2 were first recirculated at a volumetric flow rate of 1.2 L/min in the dark for 5 min. The time will be enough to reach the equilibrated adsorption of the dyestuffs on immobilized TiO_2 as a thin film within the reactor. The UV lamps (BL-B, UV-B, GL-6, UV-C and O_3-L) were respectively switched on 30 min prior to the 5 min dark of adsorption to standardize the amount of energy of UV rays that each lamp emits. The reactions were started by re-switching on the UV lamps in the reactor, respectively. Oxygen gas was not supplied to the process. The temperature effect was also negligible. Because the studies were carried out at temperatures ranging from 4–45°C. The results showed that the temperature through the photocatalytic reactor had no effect on the decolorization performance; Hence, this process has a potential of both increasing degradation while also slightly reducing operation costs. An aliquot samples (5 ml) of the latter treatments were periodically withdrawn from the reservoir to determine the CPTs of each decolorization pattern.

1.3 Textile wastewater characteristics

The actual wastewater effluents were obtained from a manufacturing facility in Jiangsu Province (Wuxi, China). The effluents were highly colored due to the presence of dyes from the fiber dying process. The typical values of actual textile wastewater used for the experiment are presented in Table 1. During this study, the actual textile wastewater was centrifuged at 8000 r/min for 15 min to aid in reduction of particulates.

Table 1 Qualities of untreated textile wastewater

Parameter	Range	Mean
pH	9–10	9.5
$A_{575\ nm}$ (AU)	0.784–0.786	0.785
COD (mg/L)	400–600	500
TIC (mg/L)	80–110	95
TN_b (mg/L)	20–40	30

A: absorbance; COD: chemical oxygen demand; TIC: total inorganic carbon; TN_b: total bound nitrogen.

The photocatalytic reactor was also fed with synthesized textile wastewater consisting of PVA (2000 mg/L), trace elements (Table 2) and a mixture of three azo dyes viz. Acid Red 17, Acid Yellow 36 and Acid Orange 52. The acid dyes were supplied by Sigma Aldrich Company. Highly concentrated solution of PVA, and trace elements were prepared separately with deionized water (pH 6.6) to be jointly mixed together. Both the prepared synthetic and actual wastewater effluents were stored at 4°C to avoid degradation. The principle of the former wastewater synthesis was to make a composite effluent with difficult photodegradable materials, including the acid dyes. A mixture of three azo dyes and an anthraquinone dye (Acid Blue 45) prepared at the concentration of 50 mg/L each were respectively treated for comparison. All experiments were repeated twice independently for each colored solution.

Table 2 Basic composition of trace elements

Composition	Concentration (mg/L)	Composition (mg/L)	Concentration (mg/L)
$CoCl_2{\cdot}6H_2O$	80	$FeCl_3{\cdot}4H_2O$	80
$ZnCl_2$	2	$MnCl_2{\cdot}4H_2O$	20
$CuCl_2{\cdot}2H_2O$	1.2	$NiCl_2{\cdot}6H_2O$	2
H_3BO_4	2	EDTA	40
36% HCl	0.04	$(NH_4)_6Mo_7O_{24}{\cdot}4H_2O$	3.6

1.4 Spectrum measurements

The rates of decolorization were observed in terms of changes in the absorbance signals using a 2450 Shimadzu Corp. UV-Vis spectrophotometer, via a 1 cm quartz cells. Absorbencies for Acid Blue 45, dye mixture, synthetic and actual wastewater were measured at 606, 454, 454 and 575 nm, which all correspond to their maximum absorption wavelengths, in that order.

2 Theory

2.1 Classical mathematics model combined with a CPT theory within photocatalytic decolorization

The catalysis process studied here occurred on an immobilized thin film of TiO_2 in annular-flow photocatalytic reactor. Minute concentration of H_2O_{2FS} (24.5 mmol/L) was present before irradiation. In this process, the same first order kinetic with respect to the absorption maximum of the dye in the visible band as results from ultrasound (Tezcanli-Guyer and Ince, 2003) occurs. The degradation of color begins with the beginning of UV light exposure and proceeds as UV distribution continues. Textile dyes in a thin-film exposed to UV and immobilized TiO_2 in the presence of H_2O_{2FS} decolorize in direct proportion to the maximum value of absorbance units (AU). The value of the rate constant depends on whether the intensity is defined as irradiance or fluence rate. And it also depends on how it is measured. In this photocatalytic-chemical reaction, the UV fluence is measured as a sum of bandgap energy of the TiO_2 (E_{bg}≈3.2 eV) and oxidation potential of minute concentration of H_2O_{2FS} (E_0 = 1.78 V). The rate at which electron hole pairs forms is determined by the light sources, the distance the UV light energy travels from the surface of the lamp to the thin film of TiO_2, and the water flow rate. Generally, when a semiconductor is immobilized in thin film, the rate of the photocatalytic reaction is increased at a very high flow rate, thereby reducing the film-diffusional resistance in recirculation of the reactant fluid (Wang and Shiraishi, 2002; Wang *et al*., 2002b).

Eq.(1) is the standard form of kinetic equation.

$$\frac{\mathrm{d}}{\mathrm{d}t}A_t = -k \times A_t \tag{1}$$

Where A is the maximum absorbance of the dye in the visible band at time t, and k is the pseudo-order absorbance decay coefficient (min^{-1}).

Different frequencies of UV light result in different k(s). With respect to A_t, Eq.(2) is a solution to Eq.(1) resulting from the separation of variables for integration.

$$\int_{A_0}^{A} \frac{1}{A_t} \mathrm{d}A_t = \int_{t_0}^{t} -k \mathrm{d}t \tag{2}$$

Eq. (3) is the integrated result.

$$\ln\left(\frac{A_t}{A_0}\right) = -k \times t \tag{3}$$

Eq.(4) simplifies A_t. The pseudo-order absorbance decay coefficient k, has units of min^{-1}, since $k \times t$ must be unitless.

$$A_t = A_0 \times \exp(-k \times t) \tag{4}$$

An inverse of k and CPT are the same in the present condition (CPT=k^{-1}). CPT is accountable to 90% of oscillations along the dye molecules to be oxidized while the remaining 10% representing the survival ratio. CPT has units of time (usually min with microseconds of four digits. In the decolorization experiments of individual dyes, the CPTs for Acid Orange 52 and Acid Yellow 36 were almost equal. However, as the CPTs were in microseconds of four digits, it was possible to differentiate between these two closely related dye). Replacing k in Eq.(4) with CPT results in:

$$A_t = A_0 \times \exp(-t/\mathrm{CPT}) \tag{5}$$

Solving Eq.(5) for CPT yields

$$\mathrm{CPT} = \frac{-t}{\ln\left(\frac{A}{A_0}\right)} \tag{6}$$

where CPT is the critical photonic time (min); A_0 is the original absorbance unit in the reservoir at the maximum absorption wavelength (AU); A_t is the absorbance unit of recirculated effluent at time t (AU).

2.2 Method for determination of photon efficiency

The photon efficiency ($\mathrm{PE}^{h\nu}$) is the amount of UV intensity that is required to make a 10-fold change in the CPT. In practice, $\mathrm{PE}^{h\nu}$ measures how the oscillations of dye molecules are to changes in UV frequencies. The $\mathrm{PE}^{h\nu}$ can be found by plotting CPTs as a function of specific UV frequencies on a logarithmic scale. The regression line was fitted to these data. The absolute value of the reciprocal of this line will be $\mathrm{PE}^{h\nu}$. Because pairs of lgCPT and specific UV frequency (λ) are important, the following equations can be used to produce the log-linear scale

$$\sum_{i=1}^{n} \mathrm{lgCPT}_i = y \times n + m \times \sum_{i=1}^{n} \lambda_i \tag{7}$$

$$\sum_{i=1}^{n} \lambda_i \times \mathrm{lgCPT}_i = y \times \sum_{i=1}^{n} \lambda_i + m \times \sum_{i=1}^{n} \lambda_i^2 \tag{8}$$

where y is the y-intercept of the regression line, m is the slope and n is the number of CPT-λ pairs. Applying the method of least squares to Eqs.(7) and (8) results in Eq.(9) which represents the slope of the regression line as:

$$m = \frac{n \times \sum_{i=1}^{n} (\lambda_i \times \mathrm{lgCPT}_i) - \sum_{i=1}^{n} \lambda_i \times \sum_{i=1}^{n} \mathrm{lgCPT}_i}{n \times \sum_{i=1}^{n} \lambda_i^2 - (\sum_{i=1}^{n} \lambda_i)^2} \tag{9}$$

From Eq.(9), the $\mathrm{PE}^{h\nu}$ can be found by taking the absolute value of the reciprocal of this slope:

$$\mathrm{PE}^{h\nu} = \left|\frac{1}{m}\right| \tag{10}$$

Calculating $\mathrm{PE}^{h\nu}$, the procedure for calculation is as follows: (1) construct a table to simplify the calculations for the values of $\sum_{i=1}^{n} \lambda_i$, $\sum_{i=1}^{n-1} \mathrm{lgCPT}_i$, $\sum_{i=1}^{n} \lambda_i^2$, and $\sum_{i=1}^{n-1} (\lambda_i \mathrm{lgCPT}_i)$ in each column, respectively; (2) plug these values into Eq.(9) for the slope of the regression line; (3) determine the number of CPT-λ pairs = n; (4) solve for $\mathrm{PE}^{h\nu}$ by Eq.(10).

2.3 Predicting unknown CPT_n for one frequency using $\mathrm{PE}^{h\nu}$ and CPTs for two or more different frequencies

This goal is accomplished by expanding the original equation for the slope of a log-linear regression line to include the unknown CPT_n. Consequently, Eq.(9) becomes

$$m = \frac{n \times \left(\sum_{i=1}^{n-1} (\lambda_i \times \mathrm{lgCPT}_i) + \lambda_n \times \mathrm{lgCPT}_n\right)}{n \times \sum_{i=1}^{n} \lambda^2 - (\sum_{i=1}^{n} \lambda)^2} - \frac{\sum_{i=1}^{n} \lambda_i \times \left(\sum_{i=1}^{n-1} (\mathrm{lgCPT}_i) + \mathrm{lgCPT}_n\right)}{n \times \sum_{i=1}^{n} \lambda^2 - (\sum_{i=1}^{n} \lambda)^2} \tag{11}$$

As the $\mathrm{PE}^{h\nu}$ is known from Eq.(10), we can substitute for m in Eq.(11) as

$$\frac{1}{\mathrm{PE}^{h\nu}} = \frac{n \times \left(\sum_{i=1}^{n-1} (\lambda_i \times \mathrm{lgCPT}_i) + \lambda_n \times \mathrm{lgCPT}_n\right)}{n \times \sum_{i=1}^{n} \lambda^2 - (\sum_{i=1}^{n} \lambda)^2} - \frac{\sum_{i=1}^{n} \lambda_i \times \left(\sum_{i=1}^{n-1} (\mathrm{lgCPT}_i) + \mathrm{lgCPT}_n\right)}{n \times \sum_{i=1}^{n} \lambda^2 - (\sum_{i=1}^{n} \lambda)^2} \tag{12}$$

Solving Eq.(12) for an unknown CPT_n yields

$$\mathrm{lgCPT}_n = \frac{\left(n \times \sum_{i=1}^{n} \lambda_i^2 - \left(\sum_{i=1}^{n} \lambda_i\right)^2\right) \div \mathrm{PE}^{h\nu}}{n \times \lambda_n - \sum_{i=1}^{n} \lambda_i} - \frac{n \times \sum_{i=1}^{n-1} (\lambda_i \mathrm{lgCPT}_i) + \sum_{i=1}^{n} \lambda_i \times \sum_{i=1}^{n-1} \mathrm{lgCPT}_i}{n \times \lambda_n - \sum_{i=1}^{n} \lambda_i} \tag{13}$$

where CPT_n is the theoretical CPT (min); $PE^{h\nu}$ is a photon efficiency required for a 10-fold reduction in CPTs; λ_n is the lambda at which the theoretical CPT exists (nm) and n is the number of CPT-λ pairs.

Hence, when all the values except for unknown CPT_n are known, the theoretical CPT is obtained from Eq.(13). Although this equation is somewhat complex, it can be simplified as follows: (1) specify the $PE^{h\nu}$ and its entire data set used to generate it; (2) construct a table to simplify the calculations for the values of $\sum_{i=1}^{n}\lambda_i$, $\sum_{i=1}^{n-1}\lg CPT_i$, $\sum_{i=1}^{n}\lambda_i^2$ and $\sum_{i=1}^{n-1}(\lambda_i \lg CPT_i)$, in that order; (3) determine the number of CPT-λ pairs = n, as to assure the value of λ_n; (4) apply these values to Eq.(13) in order to obtain a theoretical CPT; (5) check this value by including it in the original data set and calculate a new $PE^{h\nu}$. The new $PE^{h\nu}$ should be the same as the one given in the problem.

3 Results and discussion

3.1 Characterization of CPTs for dye decomposition in aqueous solution by classical mathematics

The work was performed on the selected samples consisting of textile dyes and measured the rates of dye decomposition during photo-excitation oxidation. It was observed that, the photocatalytic degradation of textile dyes in the presence of minute concentration of H_2O_{2FS} follows first-order kinetic law. The CPTs that predict the formation of electron-hole pairs at the constant rate during decomposition period of the dyes were calculated for each of the colored samples using a derived model of Eq.(6). The experimental means of CPTs are represented by dotted lines in Fig.2.

In a previous study, we reported results on the anaerobic UV-TiO_2 process in the absence of H_2O_{2FS}. These results were not promising with respect to photocatalytic activity of charge transfer for the formation of electron-hole pairs (Shigwedha *et al*., 2006). Consequently, the experimental data of CPTs plotted in the absence of H_2O_2 were neglected.

Nevertheless, when the decolorization kinetics of two or more colored solutions (or their chroma in wastewater) is analyzed by CPTs, comparison effect on their absorbance units becomes negligible. In the current formulation models, the absorbance units varied in a range of 0.785 to 2.182 AU. Knowing the dye concentrations of the samples is not crucial because the maximum absorbance units represented the initial dyes concentrations. Although Spadaro *et al*. (1993) have cautioned that the structure and concentration of individual dyes for textile industry effluent should be known before the effluent is treated using a process which relies on the hydroxyl radical chemistry, the present data indicate that it is not necessary and indeed there is no theoretical need for reason it should be necessary.

With the UV intensity below 400 nm, the decolorization rates became more and more rapid. The latter observations were especially practical for the UV intensity at 389, 313 and 254 nm. When the UV intensity reached 254 nm, the rates of converted dyes were slightly better than predicted. These data provides evidence that CPTs determined for textile dyes effluent may be used to represent the activation of targeted structures to electron hole pairs as photocataly-

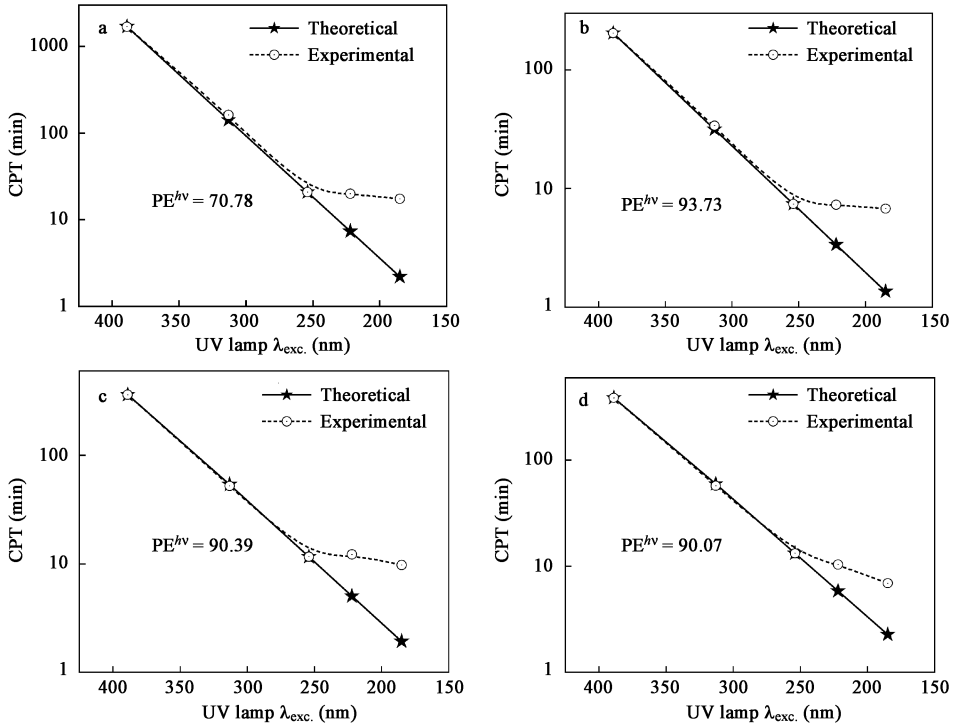

Fig. 2 Relationship between experimental CPTs and theoretical CPTs at different UV frequencies of different textile dye effluents with immobilized TiO_2 in the presence of H_2O_{2FS} (24.5 mmol/L). (a) Acid Blue 45; (b) actual textile effluent; (c) mixture of Acid Red 52 + Acid Yellow 36 + Acid Orange 52; (d) synthetic textile effluent. CPT: critical photonic time.

tic degradation proceeds. The increase in the decomposition rate as a result of the addition of H_2O_{2FS} is probably due to chain reactions caused by the attack of HO· radicals on the surface of the photocatalyst. This confirms that the addition of H_2O_{2FS} influences the state of electron-hole pairs as reported elsewhere (Shigwedha *et al*., 2006). Thus, a CPT of any UV frequency delivered by a lamp calculated as per Eq.(6) would be valid for any primary photocatalytic measurements of the organic dyes in water.

3.2 Prediction of theoretical CPT from a $PE^{h\nu}$ and known CPTs

For the present work, we formulated CPT equations not only from first-order kinetics but also from a $PE^{h\nu}$ and known CPTs. These results validated the CPT theory and expressed its practicality for a wide range of UV performance.

For a $PE^{h\nu}$ and known CPTs, the regression line represents the underlined kinetics of electron hole pairs formation by UV intensity, predicting other CPTs for the other UV intensities and validating the kinetic assumptions of the theory. All the values of CPTs along the regression line are dependent on each other. Therefore, an unknown CPT_n should fit the regression line in such a way as to not affect the decolorization kinetics, thereby not changing the value of $PE^{h\nu}$. The theoretical CPTs were determined from a $PE^{h\nu}$ and two known CPTs using the experimental data of each sample by Eq.(13) at wavelengths of 389 and 254 nm. The results are shown by solid lines in Fig.2. The relationship between the experimental CPTs and the theoretical CPTs was therefore established by these data.

The CPT model presented does not take into account possible UV fluences effects of polychromatic light sources simultaneously impinging on a $PE^{h\nu}$. These effects are expected to be minor as the activation of organic molecules at all wavelengths considered is the formation of similar results (intermediates), which are formed due to the absorbance of a single photon of light. Thus, the sum of the effects of the individual wavelengths should not be affected by the consequence of simultaneous irradiation at multiple wavelengths. A CPT obtained by a polychromatic lamp can be positioned where it fits along the regression line thereby predicting the specific wavelength within the broad spectrum. We saw specificity in the broad spectrum.

3.3 Evaluation of experimental results by mathematical models

The experimental results were consistent with the result of the theoretical investigation on the photocatalytic performances in the UV frequency between 400–254 nm. At around frequency of 222–185 nm, the results diverted as predicted by a present theory. This discrepancy is due to the UV lamp technology but not to the dyes. In the lamps of wavelength 222–185 nm, the ultraviolet ray attacked a water molecule besides it decomposes an organic compound. This is true especially when the ultraviolet rays of 185 nm is irradiated. The dissolved oxygen and water molecule are decomposed to produce the HO· radicals. That is, a large amount of energy of ultraviolet rays is consumed in not only the decomposition of the organic compound but also such a solvent reaction. The decomposition of H_2O_2 produces HO· radical, which would lead to self-digestion of H_2O_2. This may also reduce the rate of photocatalytic degradation. Therefore, it is natural that the theory does not correspond to the experimental values in such a short wavelength region. Moreover, the low-pressure mercury discharge classes of lamps produce virtually all of their UV output at a wavelength of 253.7 nm (UV_{254}), which just happens to be very close to the maximum peak germicidal effectiveness curve of 260 nm (Kurovaara *et al*., 1995). This also suggests that predicting CPTs at around 260 nm and below will have slight variations. We modeled this order-fact mathematically, because most of these low-pressure classes of lamps generally can convert up to 40% of their input watts into usable UV-C watts. To be precise, a 6-W low-pressure lamp around 254 to 185 nm will have approximately 2.5 W of UV-C power. The intensity of the light below 254 nm in UV lamps is sufficiently high that, under many conditions, the TiO_2 thin film cannot absorb all of the incident photons. Thus, this radiation can cause homogeneous photolysis reactions in addition to the desired heterogeneous photocatalytic degradation process. We did not try frequencies below 185 nm because the photodegradation rate at this frequency remained almost at maximum.

3.4 Evaluation of theoretical results by mathematical models

As shown by the solid lines in Fig.2, the CPTs predicted by Eq.(13) express satisfactorily the theoretical practicality of validation in CPTs theory for a wide range of UV bandgap illumination in the presence of H_2O_{2FS}. The experimental results agree well with the theoretical CPTs when UV frequencies were between 400 and 254 nm. Experience has shown also that the most suitable and widely used UV lamp for advanced oxidation processes (AOPs) of many organic compounds is that of 254 nm. According to the dotted lines in Fig.2, the typical CPTs below UV_{254} divert from the theoretical CPTs. Now, since the $PE^{h\nu}$ only tells us about the slope of a regression line and not its y-intercept, the line can exist anywhere along the y-axis. We simply assumed that it passes through the CPT at 254 nm, a diversion wavelength. Considering that in a perfect situation all CPTs would exist on the same regression line, they would then also decrease perfectly exponentially. For this solution, we used the most basic form for the slope of this line, which is

$$m = \frac{\lg CPT_{254} - \lg CPT_n}{254 - \lambda_n} \tag{14}$$

Solving for unknown CPT_n results in

$$\lg CPT_n = \frac{(\lambda_n - 254)}{PE^{h\nu}} + \lg CPT_{254} \tag{15}$$

where CPT_n is the theoretical CPT (min); λ_n is the lambda at which the theoretical CPT exists (nm) and CPT_{254} is the CPT at 254 nm (min).

The determination of a theoretical CPT from $PE^{h\nu}$ and only one CPT is also made possible. This calculation is

easy to perform mathematically. Interestingly, both models of Eqs.(13) and (15) are different methods of numerically obtaining the theoretical CPTs, however the difference in their values is very small. This difference appears in the final digits of the microseconds and therefore would be insignificant in all cases (Table 3).

Table 3 Detailed CPT results of the two models of Eqs.(13) and (15) for Acid Blue 45

λexc.(nm)	CPT (min)	
	Eq.(13)	Eq.(15)
389	1682.7600	1682.7600
313	142.0028	142.0031
254	20.8319	20.8319
222	7.3514	7.3557
185	2.2065	2.2074

4 Conclusions

The photocatalytic decomposition of actual- and synthesized textile wastewater containing various textile dyes has been achieved by a UV-H_2O_{2FS}-TiO_2 process. The dyes decolorized gradually at a constant rate as soon as they were exposed to UV light. Irradiations were done with different light sources with photon output below 400 nm. A set of predictions that reproduce, with reasonable accuracy, theoretically and experimentally available data have been successfully developed. The results obtained suggest the CPTs procedure as an effective and efficient kinetic-measure of photocatalytic activities in textile wastewater treatment. The CPTs explain the rate of formation of electron hole pairs formed on the surface of the immobilized photocatalyst in detail. We also found that the CPT theory in photocatalysis expresses its practicality over a wide range of UV performance, including the remarkable conversions of vacuum UV spectrum into usable germicidal spectrum. Further studies on the CPTs would be helpful to aid in the development of this kinetic-measure for primary processes of photocatalysis for the textile wastewater decontamination.

Acknowledgements: The authors would like to thank Prof. Fuhimide Shiraishi at the Department of Bio-Systems Design, Bio-Architecture Center Kyushu University (Japan) for providing a TiO_2 thin film glass and UV lamps; Richard Hirsh, Li Jia and Liang Zhou for technical analysis, and gratefully acknowledge also the financial support for this study, which is part of a Scientific Research Foundation funded for the Returned Overseas Scholars, State Education Ministry.

References

Arabatzis I M, Antonaraki S, Stergiopoulos T *et al*., 2002. Preparation, characterization and photocatalytic activity of nanocrystalline thin film TiO_2 catalysts towards 3,5-dichlorophenol degradation[J]. J Photochem Photobiol A: Chem, 149: 237–245.

Bahorsky M S, Bryant D H, 1995. Textiles[J]. Wat Environ Res, 67: 544–548.

Forgacs E, Cserháti T, Oros G, 2004. Removal of synthetic dyes from wastewaters: a review[J]. Environ Intern, 30: 953–971.

Fox M A, 1991. Photoinduced electron transfer in arranged media[J]. Top Curr Chem, 159: 67–101.

Kunz A, Reginatto V, Durán N, 2001. Combined treatment using sequence *Phanerochaete Chrysosporiun*–Ozone[J]. Chemosphere, 44: 281–287.

Kurovaara M, Backlund P, Corin N, 1995. Light-induced degradation of DDT in humic water[J]. Sci Total Environ, 170: 185–191.

Malato S, Blanco J, Richter C *et al*., 2000. Optimization of pre–industrial solar photocatalytic mineralization of commercial pesticides. Application to pesticide container recycling[J]. Appl Catal B: Environ, 25: 31–38.

Medina-Valtierra J, Moctezuma E, Sánchez-Cárdenas M *et al*., 2005. Global photonic efficiency for phenol degradation and mineralization in heterogeneous photocatalysis[J]. J Photochem Photobiol A: Chem, 174: 246–252.

Noorjahan M, Reddy M P, Kumari V D *et al*., 2003. Photocatalytic degradation of H-acid over a novel TiO_2 thin film fixed bed reactor and in aqueous suspensions[J]. J Photochem Photobiol A: Chem, 156: 179–187.

Rothenberger G, Moser J, Grätzel M, Serpone N *et al*., 1985. Charge carrier trapping and recombination dynamics in small semiconductor particles[J]. J Am Chem Soc, 107: 8054–8059.

Sabin F, Turk T, Vogler A, 1992. Photooxidation of organic compounds in the presence of titanium dioxide: determination of efficiency[J]. J Photochem Photobiol A: Chem, 63: 99–106.

Serpone N, Sauvé G, Koch R *et al*., 1996. Standardization protocol of process efficiencies and activation parameters in heterogenous photocatalysis: relative photonic efficiencies ζ_r[J]. J Photochem Photobiol A: Chem, 94: 191–203.

Shigwedha N, Hua Z, Chen J, 2006. Immobilizing TiO_2 allows H_2O_2 to be present at the start and enhances the photodegradation of Acid Yellow 36 (AY-36)[J]. J Chem Eng Japan, 39: 475–480.

Shiraishi F, Nakasako T, Hua Z, 2003. Formation of hydrogen peroxide in photocatalytic reactions[J]. J Phys Chem A, 107: 11072–11081.

Spadaro J T, Isabelle L, Renganathan V, 1993. Hydroxyl radical mediated degradation of azo dyes: evidence for benzene generation[J]. Environ Sci Technol, 28: 1389–1393.

Tahiri H, Serpone N, van Mao R L, 1996. Application of concept of relative photonic efficiencies and surface characterization of a new titania photocatalyst designed for environmental remediation[J]. J Photochem Photobiol A: Chem, 93: 199–203.

Tezcanli-Guyer G, Ince N H, 2003. Degradation and toxicity reduction of textile dyestuff by ultrasound[J]. Ultrason Sonochem, 10: 235–240.

Wang C, Rabani J, Bahnemann D W *et al*., 2002a. Photonic efficiency and quantum yield of formaldehyde formation from methanol in the presence of various TiO_2 photocatalysts[J]. J Photochem Photobiol A: Chem, 148: 169–176.

Wang S, Shiraishi F, Nakano K, 2002b. Decomposition of formic acid in a photocatalytic reactor with a parallel array of four light sources[J]. J Chem Technol Biotechnol, 77: 805–810.

Wang S, Shiraishi F, 2002. Decomposition of formic acid in two types of photocatalytic reactors: effects of film-diffusional resistance and penetration of UV light on decomposition rates[J]. Eco-Engineering, 14: 9–17.

Wu F, Ozaki H, Terashima Y *et al*., 1996. Activities of lignolytic enzymes of the white rot fungus, *Phanerochaete chrysosporiun* and its recalcitrant substances degradability[J]. Wat Sci Tech, 34: 69–77.